

# EXPERIMENTAL EVALUATION OF LOW-TEMPERATURE ORGANIC RANKINE CYCLE (ORC) ENGINE COUPLED WITH CONCENTRATING PVT SYSTEM

Chrysanthos Golonis<sup>1</sup>, Dimitris Manolakos<sup>1</sup>, George Kosmadakis<sup>2</sup> and George Papadakis<sup>1</sup>

<sup>1</sup>Agricultural University of Athens, Dept. of Natural Resources and Agricultural Engineering, Athens, Greece

<sup>2</sup>Ricreation IKE, Technological Park "Lefkippos", PatriarchouGrigoriou&Neapoleos 27, 15341,AgiaParaskevi, Greece

## Abstract

A 10 kWp Concentrating (x10) PV-Thermal collectors' array produces heat at temperatures in the range of 70-90°C, which is supplied to a low temperature ORC engine designed and manufactured for this purpose. The ORC engine converts a fraction of this heat into electricity of about 2 to 3 kW with maximum thermal efficiency in the order of 4.5%, thus ameliorating the performance of CPVT system in terms of additional electricity generation. The paper deals with the presentation of field test results under real operating conditions. ORC key variables variation according to solar irradiation availability is examined towards maximizing system performance. The results show that the magnitude of electricity produced from the ORC engine is comparable to that of directly generated from the PV and the proposed configuration could be an alternative option for efficient exploitation of CPVT heat that is mostly utilized for domestic heating.

*Keywords: Solar Energy, Concentrating PV-Thermal, Organic Rankine Cycle, Scroll expander*

---

## 1. Introduction

The organic Rankine cycle (ORC) technology has become nowadays a field of intensive research and has proved to be a very promising technology for efficient conversion of low-grade heat into useful power or electricity (Desai, 2009) and (Mago et al., 2008). Some researchers (Algieri and Morrone, 2012) and (Al-Sulaiman et al., 2011) investigated the ORC for agricultural residues and biomass-based power generation and some focused on the ORC using solar energy (Kosmadakis et al., 2016). Other research works (Zhang et al., 2013) and (Wang et al., 2013) were concentrated on the ORC use for the low-grade waste heat recovery.

ORC technology is suitable for heat recovery applications of temperature even below 100 °C (Manolakos et al., 2009). At such conditions, its efficiency is rather low, usually in the range of 4-6%, but still there are cases where it can be cost effective especially for waste heat recovery. With these range of heat to power conversion efficiency ORC is still the most efficient heat to power generation technology for low temperature heat sources applications and consequently to converting heat to power from CPV-T systems where heat is available at temperatures lower than 90 °C.

Solar energy has been the fastest-growing energy sector in the last few years. Solar energy is an ideal source of energy because of its worldwide availability (Nazari et al., 2018) and has become a reliable source of power generation on the planet (Mills et al., 2004). Current solar energy generation is increasing a lot due to high investment in the area and the decreasing cost of their production. Two solar energy decentralized systems are available for electricity generation: photovoltaic solar plants (PV) and concentrated solar power plant (CSP). The efficiency of PV modules is still low, but there have been plenty of improvements in the last years. Photovoltaic cells convert the incident radiation of the sun into electrical energy without producing any pollution or noise. Concentrating Photovoltaic (CPV) technology is one of the growing among the concentrating solar energy technologies. The concentrating photovoltaic (CPV) system is one of the most efficient techniques to reduce the cost of solar electricity. The concentrating photovoltaic/thermal (CPV/T) system is an interesting technique to broaden the field of CPV technology to a higher-efficiency energy system that produces not only electricity but also heat (Bernardo, 2011) and (Ong et al., 2012). The final result of this arrangement is the combined production

of electricity and heat and a possible improvement of PV efficiency. The PV cells can convert (6%-20%) of the incident solar radiation to electricity. The rest of the solar radiation raises the cell's temperature, which causes reduction in PV's efficiency (Dubey and Tay, 2013). Integrating the PV cells with a thermal concentrating solar collector makes the PV cooling necessary to improve its efficiency.

The result of this arrangement is the combined production of electricity and heat with improved PV efficiency. CPV/T systems tend to produce low-temperature heat of less than 80 °C, which is hot enough for domestic hotwater (DHW) applications. The current work investigates experimentally the case where the heat coming from the cooling circuit of a CPV-T system is converted to electricity instead of being used for DHW purposes. The results show that additional electricity of comparable magnitude to that produced directly from CPV-T cells can be produced with this configuration. It is stressed that the ORC engine has been constructed so that to operate also in supercritical conditions so that to investigate the potential increase power generation in this mode, however in this paper operation results from subcritical operation are provided.

## 2. Description of the system

Figure 1 shows the CPV-T-ORC system layout and a picture of the experimental installation. The solar field has been installed at the campus of the Agricultural University of Athens (AUA), in Greece. Each collector has an electric capacity of 1 kWp, concentration ratio of around 10, and the nominal heat production is of the order of 4.1 kWth. The aperture area of each collector is 10.4 m<sup>2</sup>. An overview of the CPV-T field is shown in fig. 2. Figure 3 illustrates the ORC engine and its key components.

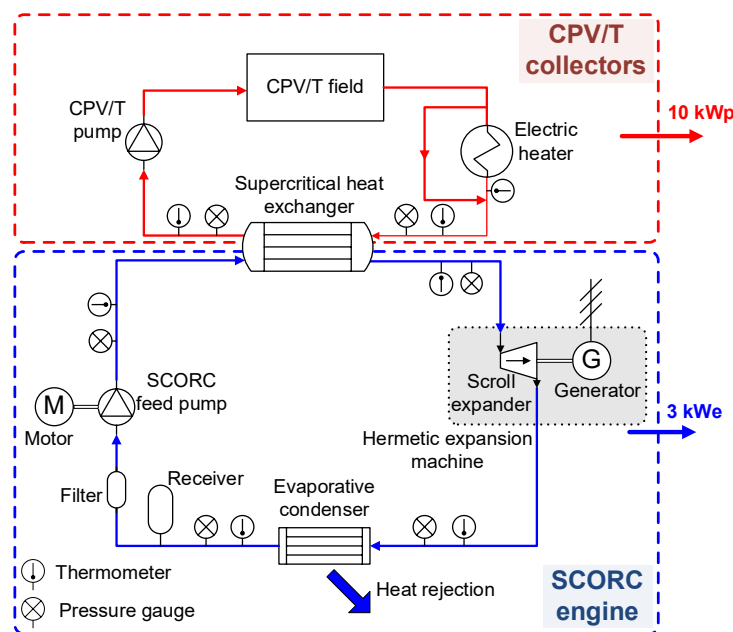


Fig. 1: Schematic representation of CPV-T coupled with ORC system and the experimental installation

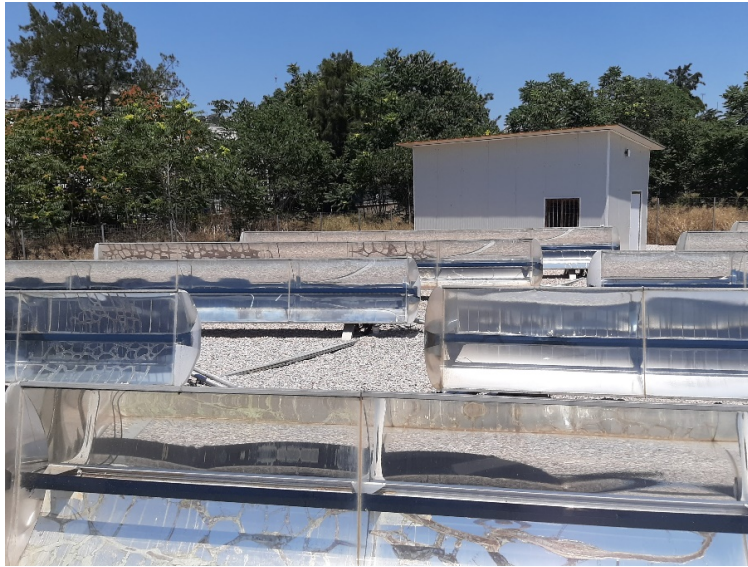


Fig. 2: The CPV-T of 10 collectors installed and the ORC engine house

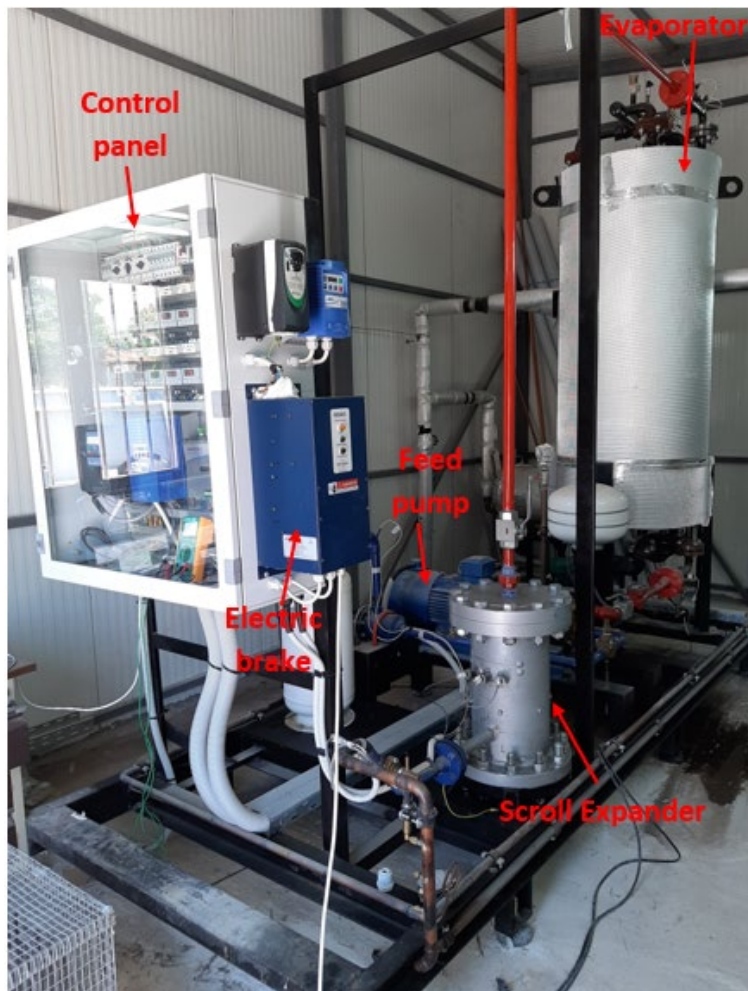


Fig. 3: The ORC engine

The key components of the ORC engine are depicted in Figs. 1 and 3, which are the following:

- The ORC pump: it is a triplex diaphragm pump manufactured by Hydra Cell (model G-10X), coupled with a 3 kW induction motor, driven by a 4 kW frequency inverter.
- The expander: it is a modified (to operate reversely) commercial scroll compressor, (Copeland ZP137KCE-TFD with swept volume of 127.15 cm<sup>3</sup>/rev., maximum isentropic efficiency 75.2%, and built-in volume ratio of around 2.8 at compressor mode). A new casing was constructed to sustain the high pressures to allow the supercritical operation as well.
- The evaporator: it is of helical coil type with a capacity of 41 kW. This helical coil heat exchanger is designed and manufactured specifically for such ORC installation, suitable to operate at relatively high pressure and temperature (capable for both sub and supercritical working conditions).
- The evaporative condenser: it is of 75 kW heat capacity (Condensing 36°C / Wet-bulb temperature 21°C) and airflow rate of 10,500 m<sup>3</sup>/h.

For small-scale systems with power production lower than around 20 kW, scroll expanders have been widely used and showed adequate performance and expansion efficiency (Lemort et al. 2012). Manolakos et al. (2009) have also used the same expansion technology (both open drive and hermetic ones) and revealed the good performance at a wide range of pressure ratios. This brings confidence that such an expander can be also used at a supercritical cycle, which is the next step of this research. One positive aspect is that for low temperature applications, the pressure ratio is low and usually in the range of 2-4 (Kosmadakis et al. 2015) enabling the scroll expander to operate with good efficiency. An electric brake (heavy duty unit, manufactured by Bonitron), is connected to the frequency inverter of the expander's induction motor, to control the test conditions and evaluate the performance of this expansion machine.

The organic fluid selected is R-404a after screening many potential fluids using environmental (zero ODP, moderate GWP) and cost criteria. It is stressed that the ORC engine is supposed to operate also in supercritical mode and R-404a is suitable under the temperature regimes imposed by the CPVT (max. temperature ~90 °C). When operating at low temperature, the condenser also becomes an important component, since thermal efficiency becomes highly sensitive to the temperature of the heat rejection medium.

### 3. Processing of measured data

For the evaluation of the system, key variables are systematically measured using appropriate instruments for both the CPV-T and the ORC engine.

#### i. CPV-T

The efficiency  $\eta_{col}$  of the collectors' array is given by the equation below:

$$\eta_{col} = \frac{\dot{Q}_{ev,col}}{A_c \cdot G_{b,n}} \cdot 100 \quad [\%] \quad (\text{eq. 1})$$

Where  $A_c$  [m<sup>2</sup>] is the collectors' aperture area,  $\dot{Q}_{ev,col}$  [kW] the heat generated by the collectors and  $G_{b,n}$  the direct normal solar irradiance.  $G_{b,n}$  is derived by multiplying the direct irradiance  $G_b$  with the  $\cos(\theta)$ , where  $\theta$  [rad], is the angle of incidence on the collectors' surface (eq. 2).

$$G_{b,n} = G_b \cdot \cos(\theta) \quad [\text{kW/m}^2] \quad (\text{eq. 2})$$

For horizontal E-W axis with N-S tracking collector,  $\cos(\theta)$  is defined as:

$$\cos(\theta) = \sqrt{1 - \cos^2(\delta) \cdot \sin^2(\omega)} \quad [-] \quad (\text{eq. 3})$$

Where  $\delta$ [rad] is the declination of the sun and  $\omega$ [rad] the angle hour.

$G_b$ , is calculated as the difference of total solar irradiance on the collectors' surface  $G_{t,track}$ [kW/m<sup>2</sup>], minus the amount of diffuse irradiance  $G_d$  [kW/m<sup>2</sup>]:

$$G_b = G_{t,track} - G_d \quad [\text{kW/m}^2] \quad (\text{eq. 4})$$

From the above equations it is concluded that  $G_{t,track}$  and  $G_d$  should be known to determine  $G_b$ . For that, two pyranometers are used. A typical pyranometer is mounted on the collectors' surface to measure the total irradiance ( $G_{t,track}$ ), while a second with shadow ring (Kipp&Zonen, CM 121) is used for directly measuring the diffuse irradiance at horizontal level ( $G_d$ ).

Finally, the quantity  $\dot{Q}_{ev,col}$  is provided by the formula below:

$$\dot{Q}_{ev,col} = \dot{m}_{col} \cdot c_p \cdot (T_{ev,col,in} - T_{ev,col,out}) \quad [\text{kW}] \quad (\text{eq. 5})$$

$T_{ev,col,in}$  and  $T_{ev,col,out}$  [°C] are the inlet and outlet temperatures at the evaporator hot (collectors') side. Thermocouples are used to measure these temperatures. To measure the mass flow rate in the collectors' circuit  $\dot{m}_{col}$  [L/s] a doppler flow meter is used.

ii. *ORC engine*

The heat supplied to the ORC engine  $\dot{Q}_{ev,orc}$  is expressed as:

$$\dot{Q}_{ev,orc} = \dot{m}_p \cdot (h_{ev,orc,out} - h_{ev,orc,in}) \quad [\text{kW}] \quad (\text{eq. 6})$$

$h_{ev,orc,out}$  and  $h_{ev,orc,in}$  [kJ/kg] are the enthalpies at the outlet and inlet of the cold (ORC') side of evaporator. These properties are defined through measuring temperature and pressure at the inlet and outlet of the evaporator using appropriate temperature and pressure transducers.  $\dot{m}_p$  [kg/s] is calculated indirectly, through the rotation speed of the ORC feed pump that is a diaphragm pump, is free of volumetric losses and thus rotation speed is linearly related with the mass flow rate.

The net power  $P_{net}$  of the ORC engine is:

$$P_{net} = P_{e,act} - P_{p,act} \quad [\text{kW}] \quad (\text{eq. 7})$$

$P_{e,act}$  and  $P_{p,act}$ [kW] are the actual power produced by the expander and absorbed by the pump respectively. Both are directly measured with appropriate instruments (kW-meters).

Finally, the thermal efficiency  $\eta_{th}$  of the ORC engine is expressed as:

$$\eta_{th} = \frac{P_{net}}{\dot{Q}_{ev,orc}} \cdot 100 \quad [\%] \quad (\text{eq. 8})$$

#### 4. Results and discussion

The experimental facility has been designed to assess the ORC engine at both subcritical and supercritical conditions, however in this work, sets of experimental results at strongly diversified subcritical operation conditions are provided once the ORC unit is supplied with heat produced by the solar field, while future work regards supercritical operation as well. Figures 4 and 5 show the variation of key variables (thermal efficiency and power generated) as function of the rotational speed of the expander when the fluid pump rotational speed is set at 864 RPM (45 Hz), when heat is supplied by the CPV-T field. As can be extracted from Fig. 4, thermal efficiency exhibits the highest values in the order of 4.5% at 2000 RPM while heat supply varies within the range of 50-52 kWth. The maximum net power generation is calculated by subtracting the power consumed by the pump from that produced by the expander. A maximum of 2.5 kW<sub>el</sub> at 2000 RPM is observed (see Fig. 3). It is stressed that the direct electricity generation from the CPVT in this condition is about 4-6 kW thus the electricity added by the ORC is about 50%.

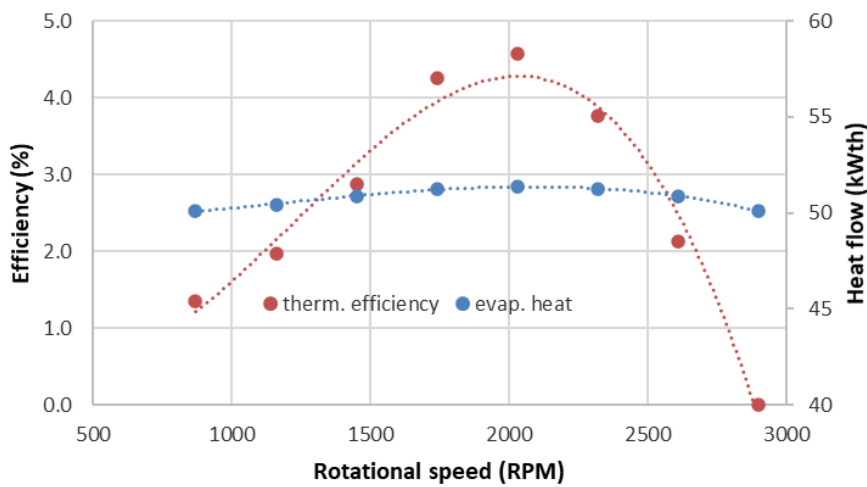


Fig. 4: Variation of thermal efficiency and heat supply at different rotation speed of expander and pump speed at 864 RPM

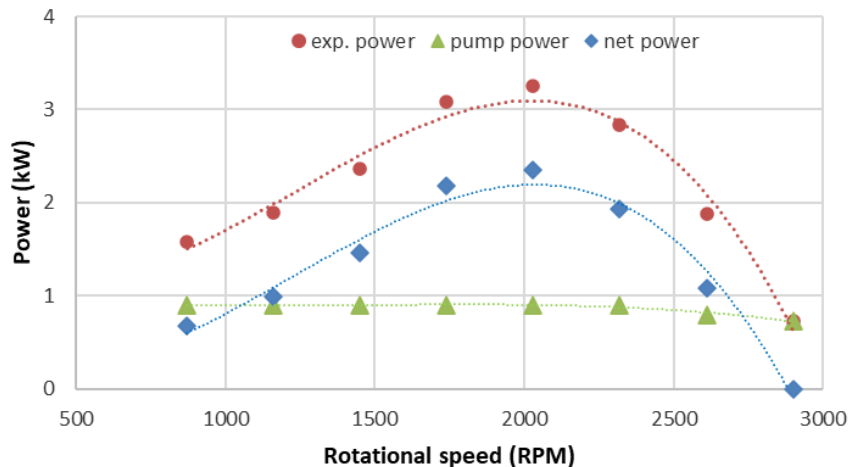


Fig. 5: Variation of power generated by the expander, power absorbed by the pump and net power at different rotation speed of expander and pump speed at 864 RPM

Other key variables that are calculated and assessed for each operating condition are the isentropic efficiencies of the pump and the expander, the pressure ratio and the filling factor of the expander. Also, the performance of the CPV-T array in all operating conditions is evaluated. Diagrams similar to the above ones provided for 864 RPM are generated for other values of pump's rotation speed and thus a complete mapping of the ORC engine operation at different heat inputs is achieved.

Next, the variation of selected key parameters is presented during the 4th of July 2020 as function of solar time. It was mostly a clear day with some cloudy intervals appearing late in the afternoon. Figure 6 shows the variation of total, direct and direct normal irradiance on collectors' surface as well as the variation of diffuse irradiance. Maximum values of the total irradiance in the order of 1000 W/m<sup>2</sup> are measured while diffuse radiation ranges between 70 and 90 W/m<sup>2</sup>. Direct normal irradiance is the fraction of total irradiance exploited from the collectors' array experiences a maximum in the order of 900 W/m<sup>2</sup> around noon and afternoon.

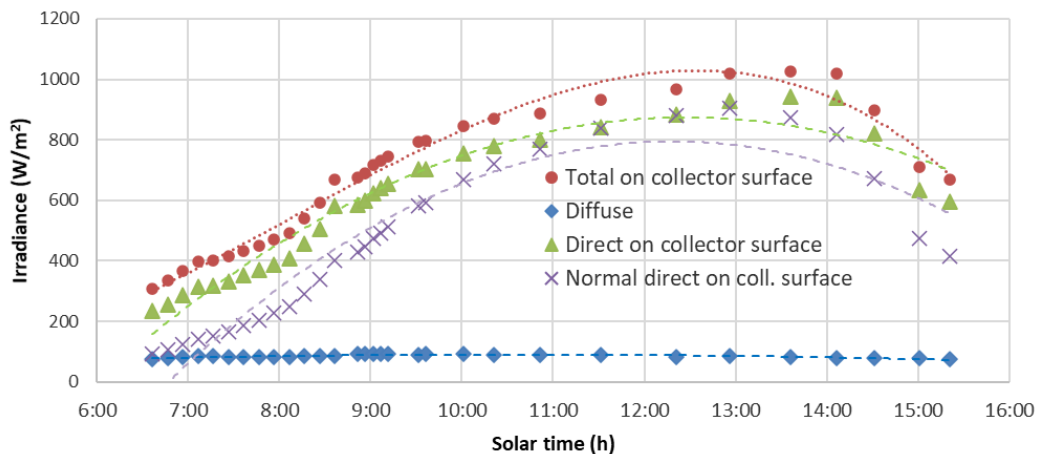


Figure 6: Total, direct, direct normal and diffuse irradiance

Figure 7 shows the variation of the inlet and outlet temperatures in the hot side of the evaporator. A maximum inlet temperature in the order of 85-88 °C is reached at around 10:00 and slightly varies until 14:00. Afterwards, a decrease of temperature is noticed as the outcome of the reduced heat gain of the collectors' field. The ORC engine operation starts at around 8:30 and hot water temperature linearly increases up to 10:00. Before 8:30 heat generated by the solar collectors' field is used to preheat the water in the collectors' circuit till its temperature reaches about 54 °C which is, the temperature threshold for the ORC engine to start operating (see also fig.8 which details this process). The inlet-outlet temperature difference variation is restricted to few degrees for most of the daily operation. In the beginning of the ORC engine operation, there is a notable increase of this difference (see Figure 9), since this heat is used to increase the temperature of the evaporators components in the ORC side.

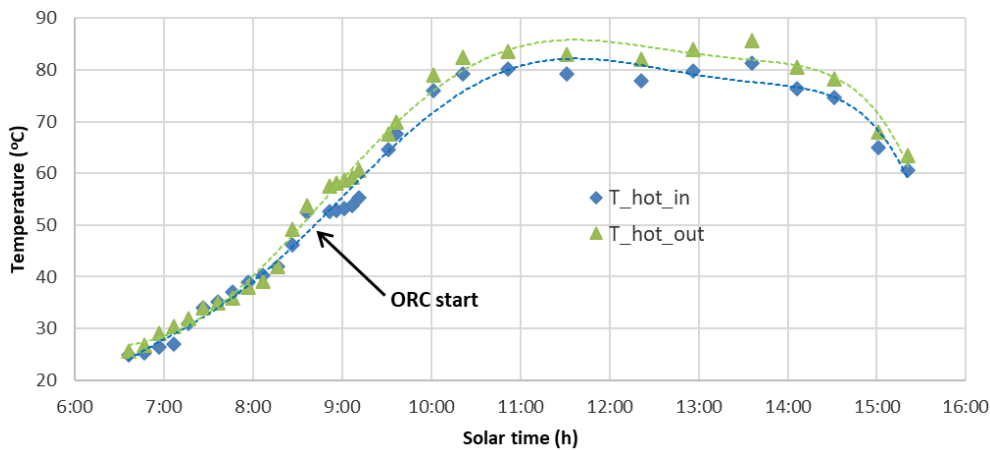


Figure 7: Inlet-outlet temperature of heating water in the evaporator

The processes taking place from the sunrise till the operation of ORC engine is stabilized at the design operation temperature (85 to 90 °C), are of specific interest and they are analyzed more extensively below. Figure 8 illustrates the temperature variation at the evaporator inlet (hot side) and the heat supplied to the working fluid (water). ORC engine is out of operation until collectors' water is heated up to the appropriate temperature, that according to the experience is of the order of 55 °C. ORC engine operation starts at around 8.30 a.m. where the water temperature is about 54 °C. Cumulatively, the collectors' array has produced about 250 MJ of heat till the engine start.

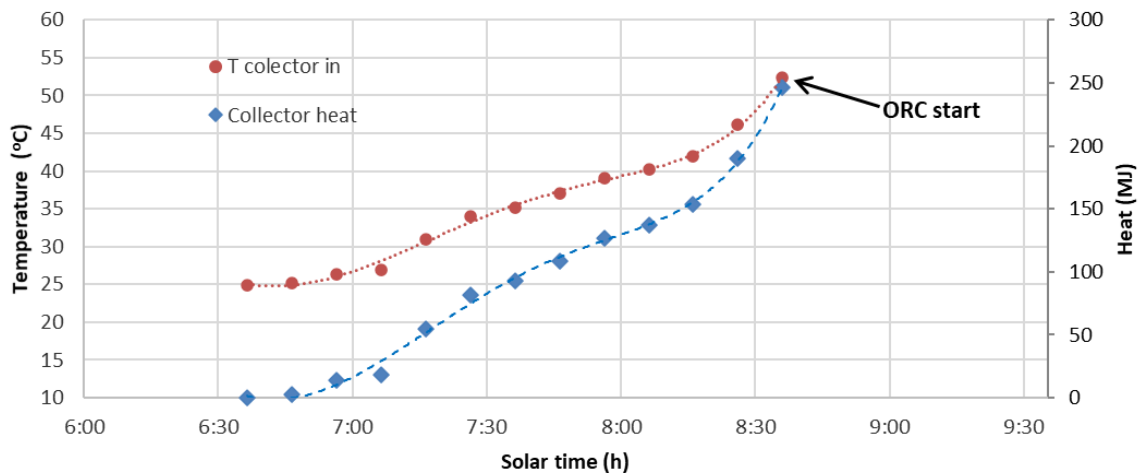


Figure 8: Elevation of temperature and heat at the collectors' array outlet until the engine start

In Figure 9 where the variation of heat flow in the hot (collectors) and cold (ORC) sides of the evaporator is depicted, throughout the ORC operation. In the beginning, the amount of heat is exchanged between the hot (collectors) and cold (ORC) sides of the evaporator to heat up the machinery and the organic fluid of ORC. It escalates fast, and within 15 min reaches to a maximum of 85 kW, while then declines till finally the operation is stabilized, as extracted from the smooth variation of heat flow curves. In the same figure, it is also observed that evaporator losses are considerable. In fact, the heat losses are measured in the range of 16-20 kW, that depending on the operation condition may represent 25 to 50% of the total heat generated. The reason is the high amount of heat being exchanged with the ambient due to the large area of the heat exchanger. Improvement of the insulation could improve the situation to some extent.



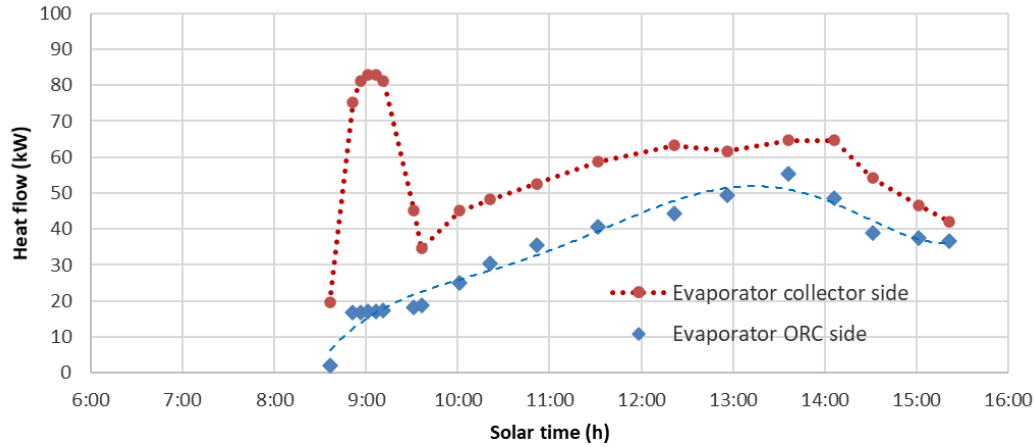


Figure 9:

Heat flow in the ORC evaporator's sides

Figure 10 shows the variation of the thermal efficiency of the ORC engine. It is clearly shown that minimum values in the order of 1.5 to 2% are observed at the beginning of the operation. Then the thermal efficiency is gradually increasing and reaches its maximum of about 4-4.5% between 10:00 to 14:00. Following the reduction of the solar irradiance, thermal efficiency starts to decrease till the system stops operating at about 15:30. The ORC operates at partial load in that case and this is also reflected to the thermal efficiency. The solar collectors' efficiency varies from 52 to slightly above 60% with the upper value to be observed around solar noon.

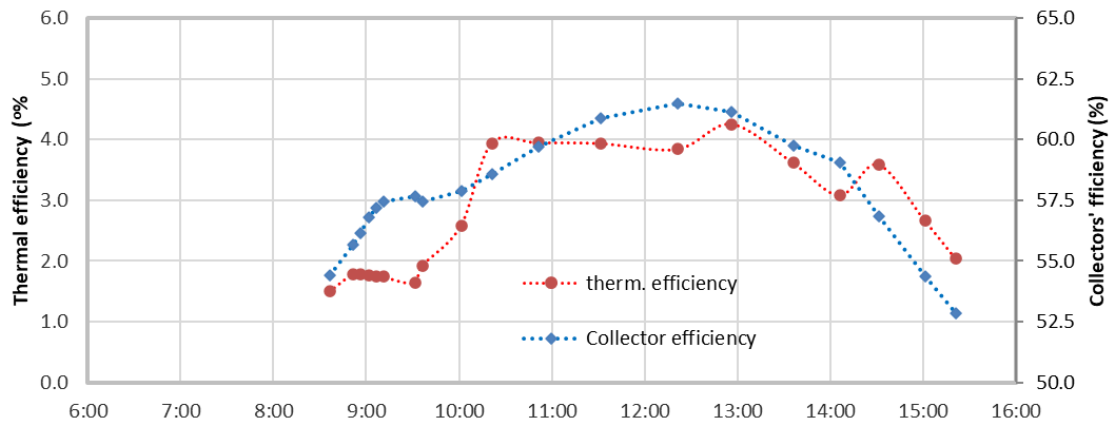


Figure 10: Collectors' and ORC thermal efficiency

Figure 11 presents the variation of expander, pump and net power during the day. Net power experiences low values in the beginning of ORC operation, and then it follows the trend of solar irradiance (Fig. 6). A maximum value slightly above 2 kW is noticed when the solar irradiance is maximized while in the afternoon the net power gradually decreases. This is comparable to the electricity produced directly by the PV cells that varies in the range of 4-6 kWe.

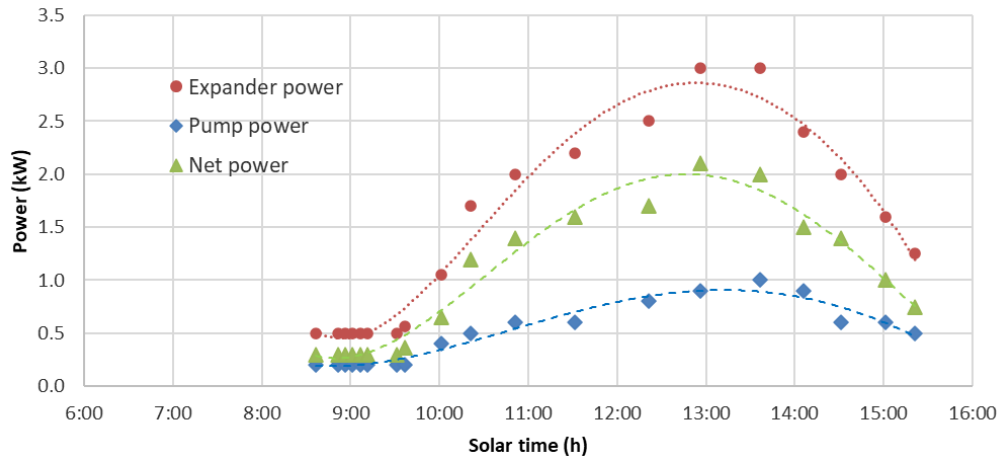


Figure 11: Expander's, pump and net power

After 15:30, the system experiences a radical decrease of net power generation due to the drop of direct normal solar irradiance, resulting from the increase of the angle of incidence and clouds (see fig. 6).

## 5. Conclusions

The integration of an ORC engine to a CPV-T array was investigated with the purpose of using the heat of the cooling circuit to generate additional electricity. The results prove that the coupling of ORC in CPVT systems is a reliable alternative of exploiting the heat production and thus generate additional electricity. In fact, ORC is capable to produce electricity comparable to that being directly offered by the PV cells, since the ORC engine power generation reached 2 kWe while the electricity generation of the CPV ranges from 4-6 kWe. Around solar noon, the ORC engine experienced the higher thermal efficiency, around 4.5%. This value is fair for ORC operating at top temperatures in the order of 80-85 °C. The integration of an ORC engine can add flexibility in CPV-T systems application since DHW is seasonally or even daily dependent. Thus, ORC could offer a solution towards diversification in CPV-T heat exploitation that finally can affect effectively to their economic viability.

## 6. Acknowledgments

The research leading to these results has received funding from the European Union's Seventh Framework Programme managed by REA-Research Executive Agency, under grant agreement no. 315049 [CPV/RANKINE], FP7-SME-2012.

## 7. References

- Algieri A. and Morrone P., 2012. Comparative energetic analysis of high-temperature subcritical and transcritical organic Rankine cycle (ORC). A biomass application in the Sibari district. *Appl. Therm. Eng.* 36, 236–244.
- Al-Sulaiman F. A., Hamdullahpur F., and Dincer I., 2011. Greenhouse gas emission and exergy assessments of an integrated organic Rankine cycle with a biomass combustor for combined cooling, heating and power production. *Appl. Therm. Eng.* 31, 439–446.
- Bernardo, L. R., Perers, B., Hakansson, H. and Karlsson, B., 2011. Performance evaluation of low concentrating photovoltaic/thermal systems: A case study from Sweden. *Sol. Energy*, 85, 1499-1510.
- Desai NB, Bandyopadhyay S., 2009. Process integration of organic Rankine cycle. *Energy*. 34(no.10):1674-86.
- Dubey S, Tay A., 2013. Testing of two different types of photovoltaic-thermal (PVT) modules with heat flow pattern under tropical climatic conditions. *Energy Sustain Dev.* 17:1-12.

- Kosmadakis G, Landelle A., Lazova M., Manolakos D., Kaya A., Huisseune H., Karavas C., Tauveron N., Revellin R., Haberschill P., De Paepe M., Papadakis G., 2016. Experimental testing of a low-temperature organic Rankine cycle(ORC) engine coupled with concentrating PV/thermal collectors:Laboratory and field tests,Energy. 117, 222-236.
- Kosmadakis G, Manolakos D, Papadakis G. 2015. An investigation of design concepts and control strategies of a double-stage expansion solar organic Rankine cycle. *Int J Sustain Energy*.34(7):446-67.
- Lemort V, Declaye S, Quoilin S.,2012. Experimental characterization of a hermetic scroll expander for use in a micro-scale Rankine cycle. *Proc Inst Mech Eng A J Power Energy*. 226(1):126-36
- Mago PJ, Chamra LM, Srinivasan K, Somayaji S., 2008. An examination of regenerative organic Rankine cycles using dry fluids. *Appl ThermEng*. 28:998-1007.
- Manolakos D, Kosmadakis G, Kyritsis S, Papadakis G.,2009. Identification of behavior and evaluation of performance of small scale, low-temperature organicRankine cycle system coupled with a RO desalination unit. *Energy*. 34(6):767-774.
- Mills, D., 2004. Advances in solar thermal electricity technology. *Solar Energy*. 76 (1–3), 19–31.
- Mosaddek H, AHMR Sazedur, Afsana SK, Faruque MMH, Shoeb A., 2017. Systematic assessment of the availability and utilization potential of biomass in Bangladesh. *Renew Sustain Energy Rev*. 67:94–105.
- Nazari MA, Aslani A, Ghasempour R.,2018. Analysis of solar farm site selection based on TOPSIS approach. *IJSESD*. 9(1):12–25.
- Ong, C. L., Escher, W. S., Paredes, A. S., Khalil, G. and Michel, B., 2012. A novel concept of energy reuse from high concentration photovoltaic thermal (HCPVT) system for desalination. *Desalination*, 295, 70-81.
- Othmana M.Y., B. Yatima, Sopianb K., Abu Bakara M.N., 2007. Performance studies on a finned double-pass photovoltaic-thermal (PV/T) solar collector, *Desalination*, 209, (1-3), 43–49.
- Wang D., Ling X., Peng H. , Liu L., and Tao L., 2013. Efficiency and optimal performance evaluation of organic Rankine cycle for low grade waste heat power generation, *Energy* 50, 343–352.
- Wang D., Ling X., and Peng H., 2012. Performance analysis of double organic Rankine cycle for discontinuous low temperature waste heat recovery. *Appl. Therm. Eng*. 48, 63–71.
- Zhang H. G., Wang E. H., and Fan B. Y., 2013. A performance analysis of a novel system of a dual loop bottoming organic Rankine cycle (ORC) with a light-duty diesel engine, *Appl. Energy*. 102, 1504–1513.